phys. stat. sol. (b) **242**, No. 7, 1406–1413 (2005) / **DOI** 10.1002/pssb.200440019

Quantum Monte Carlo approach to the Holstein polaron problem

Martin Hohenadler*, **Hans Gerd Evertz,** and **Wolfgang von der Linden**

Institute for Theoretical and Computational Physics, Graz University of Technology, Petersgasse 16, 8010 Graz, Austria

Received 21 December 2004, revised 16 February 2005, accepted 23 February 2005
Published online 11 April 2005

PACS 2.70.Ss, 63.20.Kr, 71.27.+a, 71.38.Ht

A recently developed quantum Monte Carlo approach to the Holstein model with one electron [Phys. Rev. B **69**, 024301 (2004)] is extended in several aspects. In addition to a straight-forward generalization to higher dimensions, a checkerboard breakup for the hopping part of the Hamiltonian is introduced, which allows significantly faster simulations. Moreover, results are extrapolated towards the limit of continuous imaginary time to remove the error due to the Trotter–Suzuki approximation. The performance and accuracy of the current approach are compared to existing quantum Monte Carlo methods. To demonstrate the applicability of our method for almost arbitrary parameters, we study the small-polaron crossover in one to three dimensions by calculating the electronic kinetic energy.

1 Introduction

In recent years, a lot of experimental evidence has been given for the importance of electron–phonon interaction in strongly correlated systems such as the cuprates [1] or the manganites [2]. Although considerable theoretical progress has been made in understanding and describing many details of the physics of these compounds, the quantum nature of the phonons has often been neglected in actual calculations [3, 4]. However, a quantum-mechanical treatment of the lattice degrees of freedom has been shown to give significantly different results in certain parameter regimes [2].

Due to the complexity of the models for the above-mentioned classes of materials, and the absence of exact analytical results, numerical methods have been used extensively. One very powerful approach is the quantum Monte Carlo (QMC) method, which allows simulations on relatively large lattices and gives quasiexact results (i.e., exact apart from statistical errors which can be systematically reduced) also at finite temperature. The latter point represents a major advantage over, e.g., the density matrix renormalization group (DMRG) or exact diagonalization (ED) – usually restricted to the calculation of ground-state properties at least for the parameters of interest – since fascinating phenomena such as high-temperature superconductivity and colossal magnetoresistance can be investigated. Additionally, for coupled electron–phonon systems, the infinite-dimensional Hilbert space of the boson degrees of freedom represents a substantial difficulty for ED and DMRG, in contrast to QMC. Despite these advantages, QMC methods are often limited by (1) the minus-sign problem, restricting simulations to high temperatures and/or small systems, (2) the fact that the calculation of dynamical properties, such as the one-electron Green function, requires analytic continuation to the real-time axis which is an ill-posed problem, and (3) by strong autocorrelations and large statistical errors.

In a recent paper [5], we have proposed a new QMC approach to the Holstein model, which is based on the canonical Lang–Firsov transformation [6] and a principal component representation of the phonon

* Corresponding author: e-mail: hohenadler@itp.tu-graz.ac.at

degrees of freedom. The resulting algorithm completely avoids the problem of autocorrelations and strongly reduces statistical errors [5]. The aim of this work is to extend this method to more than one dimension and to improve its accuracy and performance by suitable modifications. This includes the extrapolation of results to remove the Trotter discretization error, and the use of a checkerboard breakup for the hopping term. In contrast to some existing approaches, the method thus obtained yields very accurate results over an extremely large range of the electron–phonon interaction strength and the phonon frequency, especially in the important adiabatic regime of small phonon frequencies realized in many polaronic materials. Moreover, owing to the reduced computer time, finite-size effects can be minimized by using larger clusters. Although we shall present some results for the small-polaron crossover, this paper is rather methodological in character.

The single polaron case (the *Holstein polaron problem*) considered here is expected to apply to semiconductors with low carrier density and doped insulators (see, e.g., [7]). While the understanding of the model with one electron is fairly complete, the present algorithm can also be applied to the challenging many-electron problem [8], and to the Holstein–Hubbard model with two electrons [9]. Although single-polaron models are frequently used to describe strongly correlated materials such as the manganites [2], the principle shortcomings of such approaches have recently been illustrated [8] (see also [2]).

The paper is organized as follows. In Section 2 we review previous work, while in Section 3 we briefly discuss the QMC method introduced in [5]. Results are presented in Section 4, and Section 5 contains our conclusions.

2 The Holstein model

The Holstein Hamiltonian [10] with dimensionless phonon variables reads [5]

$$H = \underbrace{-t \sum_{\langle i,j \rangle} c_i^\dagger c_j}_{K} + \underbrace{\frac{\omega}{2} \sum_i \left(\hat{p}_i^2 + \hat{x}_i^2 \right)}_{P} \underbrace{-\alpha \sum_i \hat{n}_i \hat{x}_i}_{I} , \tag{1}$$

where we have introduced the abbreviations K, P and I for the kinetic, phonon and interaction terms, respectively. Owing to the spin symmetry of the one-electron problem, a spin index has been suppressed, resulting in a model of spinless fermions. In Eq. (1), $c_i^\dagger (c_i)$ creates (annihilates) a spinless fermion at lattice site i, $\hat{x}_i (\hat{p}_i)$ denotes the displacement (momentum) operator of a harmonic oscillator at site i, and $\hat{n}_i = c_i^\dagger c_i$. The coupling term I describes the local interaction of the single electron considered here with dispersionless Einstein phonons. In the first term, the symbol $\langle i, j \rangle$ denotes a summation over all hopping processes between neighboring lattice sites i, j. The parameters of the model are the hopping integral t, the phonon energy ω ($\hbar = 1$), and the electron–phonon coupling constant α. We define the dimensionless coupling constant $\lambda = \alpha^2/(\omega W)$, where $W = 4tD$ is the bare bandwidth in D dimensions. We shall also use the dimensionless phonon frequency $\bar{\omega} = \omega/t$, often called the "*adiabatic ratio*", and express all energies in units of t. Consequently, the model can be described by two independent parameters, $\bar{\omega}$ and λ. Periodic boundary conditions in real space have been applied.

Since the literature on the Holstein polaron problem is vast, we restrict our discussion to work in more than one dimension, while the 1D case has been reviewed in [5]. Moreover, we will focus on recent progress in the field, and on numerical methods. A comprehensive overview of earlier analytical work can be found, e.g., in the books of Alexandrov and Mott [11] and Mahan [12]. The Holstein polaron in $D > 1$ has been studied using a large variety of numerical techniques. In contrast to many perturbative approaches [11, 12], the latter can also accurately describe the physically most interesting regime of small but finite phonon frequency ($0 < \bar{\omega} < 1$) at intermediate-to-strong electron–phonon coupling ($\lambda \approx 1$). Much information about the Holstein polaron has been obtained using QMC. De Raedt and Lagendijk [13–15] applied Feynman's path-integral technique to the lattice problem of Eq. (1), by integrating out analytically the phonon degrees of freedom. The only approximation of this method – applicable for one or two electrons only – consists of a Suzuki–Trotter discretization of the imaginary time [14]. As the

phonons have been completely eliminated from the problem, accurate simulations on large lattices even in higher dimensions are possible [13–16]. Extending this work, Kornilovitch developed a QMC approach formulated in continuous imaginary time and on an infinite system, which is capable of directly measuring the polaron band dispersion $E(k)$ and the density of states [17, 18]. Although the method gives very accurate results and can also be applied to more general models with, e.g., long-range interaction, it is limited to the regime of intermediate and strong electron–phonon coupling as well as $\bar{\omega} \gtrsim 1$ by a minus-sign problem [17, 18]. Similar to the present approach, the methods of [13–16] are free of autocorrelations but, unfortunately, cannot be extended to the important many-electron case. The same seems to be true for the diagrammatic QMC approach [19, 20].

Apart from QMC, several other methods have been successfully applied to the Holstein polaron problem. This includes ED in combination with a truncation of the phonon Hilbert space [21–23], finite-cluster strong coupling perturbation theory (SCPT) [24], cluster perturbation theory (CPT) [25], DMRG [26], and a variational diagonalization method [27]. For realistic parameters, standard ED is restricted to rather small systems, while results of DMRG (in one dimension) [26] and the variational method of [27] are only weakly influenced by finite-size effects. The same is true for SCPT and CPT, which exactly diagonalize small clusters – for which enough phonon states can be included in the calculation – and extrapolate the results to the thermodynamic limit by treating the rest of the system as a perturbation [24, 25]. Remarkably, the Holstein polaron problem has been solved exactly in infinite dimensions [28–32]. Finally, it has been investigated recently using weak- and strong-coupling perturbation theory [33, 34], and a variational approach [35].

3 Quantum Monte Carlo method

The extension of the algorithm proposed in [5] to higher dimensions is straight forward. Therefore, we shall provide only a brief review of the most important ideas, and discuss the improvements announced above.

The cornerstone of the new approach is the canonical Lang–Firsov transformation [6] with the unitary operator $\nu = \mathrm{e}^{i\gamma \sum_j \hat{n}_j \hat{p}_j}$, which removes the direct coupling term I between the electron density and the lattice displacement in Eq. (1). The transformed model with one electron takes the form [5]

$$\tilde{H} = \tilde{K} + P - E_P\,, \qquad \tilde{K} = -t \sum_{\langle i,j \rangle} c_i^\dagger c_j \mathrm{e}^{i\gamma(\hat{p}_i - \hat{p}_j)} \tag{2}$$

with P as defined in Eq. (1), and the polaron binding energy $E_P = \lambda W/2$. The parameter γ, which corresponds to the atomic-limit lattice displacement in the presence of an electron [5], is given by $\gamma^2 = 2E_P/\omega$. The method employs a Trotter decomposition of the imaginary time axis into L intervals of size $\Delta\tau = \beta/L$, where $\beta = (k_\mathrm{B}T)^{-1}$ is the inverse temperature. The resulting partition function, obtained by integrating out the phonon coordinates [5], is given by

$$Z_L = C^{NL} \int \mathcal{D}p\, w_b\, w_f\,, \qquad C = \sqrt{2\pi/\omega\,\Delta\tau}\ , \tag{3}$$

where $\int \mathcal{D}p$ denotes an LN^D dimensional integral over all phonon momenta p, and N is the linear size of the lattice in D dimensions. The bosonic weight w_b is defined by $\mathrm{e}^{-\Delta\tau S_b}$ with the bosonic action

$$S_b = \frac{\omega}{2} \sum_{i,\tau} p_{i,\tau}^2 + \frac{1}{2\omega\,\Delta\tau^2} \sum_{i,\tau} \left(p_{i,\tau} - p_{i,\tau+1}\right)^2 . \tag{4}$$

Here i and τ run over all lattice sites and Trotter times, respectively. The electronic weight w_f is given by [5]

$$w_f = \mathrm{Tr}_f\, \Omega\,, \qquad \Omega = \prod_{\tau=1}^{L} \mathrm{e}^{-\Delta\tau \tilde{K}_\tau}\,, \tag{5}$$

where $\tilde{K}_\tau$ is $\tilde{K}$ with the phonon operators $\hat{p}_i$, $\hat{p}_j$ replaced by the values $p_{i,\tau}$, $p_{j,\tau}$ on the τth Trotter slice. The exponential of the hopping term can be written as

$$\mathrm{e}^{-\Delta\tau\tilde{K}_\tau} = D_\tau \kappa D_\tau^\dagger, \qquad \kappa_{jj'} = \left(\mathrm{e}^{(\Delta\tau)t h^{tb}}\right)_{jj'}, \qquad (D_\tau)_{jj'} = \delta_{jj'}\mathrm{e}^{i\gamma p_{j,\tau}}, \tag{6}$$

where h^{tb} is the $N^D \times N^D$ tight-binding hopping matrix [36] for the lattice under consideration. In fact, this is the only nontrivial change compared to the one-dimensional case. The matrix κ is not sparse but needs to be computed only once, as it does not depend on the random phonon fields $p_{j,\tau}$.

The most time-consuming part of the simulation is the evaluation of the matrix product in Eq. (5). To reduce the computer time, we make use of the so-called checkerboard breakup of the hopping term K, which takes the form [37]

$$\mathrm{e}^{t\,\Delta\tau\sum_{\langle i,j\rangle} c_i^\dagger c_j} \approx \prod_{\langle i,j\rangle} \mathrm{e}^{t\,\Delta\tau c_i^\dagger c_j}, \tag{7}$$

and reduces the numerical effort roughly by a factor $\propto N^D$ (see Sec. 4). The error due to this additional approximation is of the same order $(\Delta\tau)^2$ as the Trotter–Suzuki error. However, using Eq. (7), the computational effort is significantly reduced, since for each pair $\langle i, j\rangle$ one is left with a 2×2 matrix.

For a single electron, the fermionic trace can easily be calculated from the $N^D \times N^D$ matrix representation of Ω as $w_f = \sum_i \Omega_{ii}$ [5]. Due to the complex-valued hopping term, w_f is not strictly positive, which gives rise to a moderate minus-sign problem. The dependence of the latter on the system parameters has been discussed in [5] for the one-dimensional case. Most importantly, we reported that it diminishes with increasing system size, and therefore does not affect simulations significantly. A similar behavior is found in higher dimensions, although the average sign reduces with increasing dimensionality for the same linear system size and parameters β, $\bar{\omega}$ and λ [38]. We would like to mention that, in contrast to standard determinant QMC methods [39], the evaluation of the L-fold product in Eq. (5) does not require a time-consuming numerical stabilization since the matrices are sufficiently well conditioned.

In [5], we have introduced the so-called principal component representation for the phonon degrees of freedom. In terms of the latter, the bosonic weight takes a simple Gaussian form, and the phonons can therefore be sampled exactly. Moreover, the efficiency of the QMC algorithm can be greatly improved by using only the bosonic weight w_b for generating phonon configurations, and taking into account the fermionic weight w_f, the evaluation of which is numerically expensive, by the use of a reweighting of the probability distribution. The calculation of observables in this case has been outlined in [5].

Due to the analytic integration over the phonon coordinates x used here, interesting observables such as the correlation functions $\sum_i \langle \hat{n}_i \hat{x}_{i+\delta}\rangle$ are difficult to measure accurately. At zero temperature, the quasiparticle weight, and the closely related effective mass [21], both of which have been used in the past to identify the small-polaron crossover (see, e.g., [27]), can be determined as the weight of the slowest-decaying exponential from the time-dependent one-electron Green function [40]. This would require an extension of the present approach to a projector QMC method [39], which is possible but has not been done here due to the existence of more accurate techniques [27]. From the one-electron Green function, and using the maximum entropy method (for a review see [41]) one can also calculate (inverse) photoemission spectra, which have recently been studied for the polaron problem using CPT [25]. In the present work, we have restricted ourselves to the kinetic energy of the electron. However, in the demanding many-electron case, an extension of the current method has recently been used to obtain comprehensive results, e.g., for the one-electron density of states and spectral function [8].

The error due to the Trotter decomposition is proportional to $(\Delta\tau)^2$ (see I). In contrast to the one-dimensional case [5], here we perform simulations at different values of $\Delta\tau$, typically $\Delta\tau = 0.1$, 0.075 and 0.05, and extrapolate results to $\Delta\tau = 0$. This is a common procedure in the context of discrete-time QMC methods [39], and allows one to remove the Trotter error if the values of $\Delta\tau$ are sufficiently small.

4 Results

The most interesting observable, which is easily accessible with our method and allows us to investigate the small-polaron crossover, is the one-electron kinetic energy $E_k = \langle K \rangle$, given by the expectation value of the first term in Hamiltonian (1). In order to compare results for different dimensions, we define the normalized quantity

$$\bar{E}_k = E_k/(-2tD) \tag{8}$$

with $\bar{E}_k = 1$ for $T = 0$ and $\lambda = 0$. Due to the large amount of work that has been devoted to the Holstein polaron in the past, we restrict ourselves to a demonstration of the capability of the present method and a brief discussion of the physics behind the small-polaron crossover. The kinetic energy of the one-electron problem has been calculated before by several authors [13, 14, 16, 22, 26, 27, 33, 34, 42].

We have fixed the inverse temperature to $\beta t = 10$, which is low enough to identify the small-polaron crossover. Calculations at even lower temperatures can easily be done for $\bar{\omega} > 1$, while similar simulations in the adiabatic regime $\bar{\omega} < 1$ require a large number of measurements to ensure satisfactorily small statistical errors. System sizes were 32 sites in $1D$, a 12×12 cluster in $2D$, and a $6 \times 6 \times 6$ lattice in $3D$. While results in one and two dimensions are well converged with respect to system size for these parameters, nonnegligible finite-size effects (maximal relative changes of up to 20% between $N = 5$ and $N = 6$ for $\bar{\omega} \ll 1$; much smaller changes otherwise) exist in three dimensions (see also Fig. 10 in [38]). Moreover, for small N, changes due to thermal population of states with nonzero momentum k – absent in ground-state calculations – are visible, as discussed below. Nevertheless, the main characteristics are well visible already for $N = 6$. A detailed study of both finite-size and finite-temperature effects can be found in [38, 43]. Error bars are always smaller than the symbol size. As pointed out before, the results shown here have been obtained by extrapolating to $\Delta\tau = 0$.

Figure 1 shows $\bar{E}_k$ as a function of the electron–phonon coupling λ for different phonon frequencies varying over two orders of magnitude, in one to three dimensions. Generally, the kinetic energy is large at weak coupling, where the ground state consists of a weakly dressed electron or a large polaron (see below). It reduces more or less strongly – depending on $\bar{\omega}$ – in the strong-coupling regime, where a small, heavy polaron exists, defined as an electron surrounded by a lattice distortion localized at the same site. The finite values of $\bar{E}_k$ even for large λ are a result of undirected motion of the electron inside the surrounding phonon cloud. In contrast, the quasiparticle weight is exponentially reduced in the strong-coupling regime (see, e.g., [27]), whereas the effective mass becomes exponentially large.

In all dimensions, the phonon frequency has a crucial influence on the behavior of the kinetic energy. While in the adiabatic regime $\bar{\omega} < 1$ the small-polaron crossover is determined by the condition $\lambda = E_P/2tD > 1$, the corresponding criterion in the nonadiabatic regime $\bar{\omega} > 1$ is $E_P/\omega > 1$. The former condition reflects the fact that the loss in kinetic energy of the electron has to be outweighed by a gain in potential energy in order to make small-polaron formation favorable. The latter condition expresses the increasing importance of the lattice energy for $\bar{\omega} > 1$, since the formation of a "localized" state requires a sizable lattice distortion. As a consequence, for large phonon frequencies, the critical coupling shifts to $\lambda_c > 1$, whereas for $\bar{\omega} < 1$ we have $\lambda_c = 1$. Additionally, the decrease of $\bar{E}_k$ at λ_c becomes significantly sharper with decreasing phonon frequency.

Concerning the effect of dimensionality, Fig. 1 reveals that, for a fixed $\bar{\omega}$, the small-polaron crossover becomes more abrupt in higher dimensions, leading to a very sharp decrease in $3D$. Nevertheless, there is no real phase transition [44]. Figure 1 also contains results for $N = 6$ in one and two dimensions, i.e., for the same linear cluster size as in $3D$ (dashed lines). Clearly, for such small clusters, the spacing between the discrete allowed momenta $\boldsymbol{k}$ is too large to permit substantial thermal population, so that results are closer to the ground state [e.g., $\bar{E}_k(\lambda = 0) \approx 1$], and exhibit a slightly more pronounced decrease near the small-polaron crossover. However, the sharpening of the latter with increasing dimensionality is still well visible (see also Fig. 11 in [38]).

We would like to point out that an interesting open question in the context of the Holstein polaron problem concerns the difference between the weak-coupling ground states in one and in higher dimen-

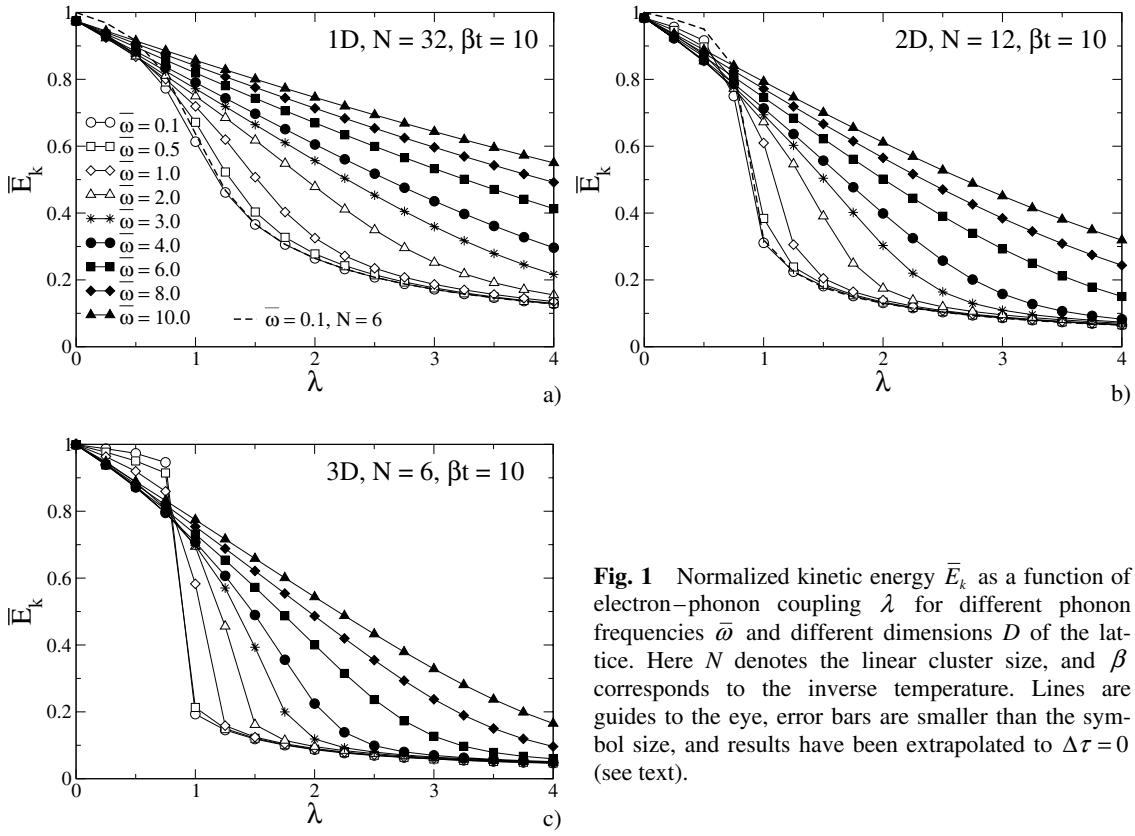

Fig. 1 Normalized kinetic energy $\bar{E}_k$ as a function of electron–phonon coupling λ for different phonon frequencies $\bar{\omega}$ and different dimensions D of the lattice. Here N denotes the linear cluster size, and β corresponds to the inverse temperature. Lines are guides to the eye, error bars are smaller than the symbol size, and results have been extrapolated to $\Delta\tau = 0$ (see text).

sions. While for 1D a large polaron – i.e., a polaron extending over more than one lattice site – is formed at any $\lambda > 0$, the electron is expected to remain quasi-free in $D > 1$ for $\lambda < \lambda_c$, and to undergo a crossover to a small polaron at λ_c [45, 46]. However, in recent studies [27, 34], authors argue that the physics of the Holstein polaron is qualitatively the same in all dimensions. Unfortunately, this issue cannot be addressed using the current approach, owing to finite-size and finite-temperature effects, and the fact that correlation functions such as $\langle \hat{n}_i \hat{x}_j \rangle$ cannot be determined accurately (see Section 3).

The results for $\bar{E}_k$ presented here agree well with existing work. Apart from small quantitative differences owing to finite-size and finite-temperature effects, the behavior of the kinetic energy is in perfect accordance with previous calculations [13, 14, 16, 22, 26, 27, 33, 34, 42]. The statistical errors of the results presented depend on $\bar{\omega}$, βt, N and λ. Away from $\lambda \approx 1$ (for $\bar{\omega} \ll 1$), error bars are use usually smaller than the line width, corresponding to relative errors of less than 0.5%. This is comparable to the accuracy of the results given by Kornilovitch [17] and significantly more accurate than the results by DRL [13, 14].

We conclude this section by comparing our approach to other QMC methods for the Holstein polaron. As mentioned in Sec. 2, the world-line methods of de Raedt and Lagendijk [13–15] and Kornilovitch [16–18] are based on an analytic integration over the phonons. This separation of electronic and bosonic degrees of freedom – particularly effective for a single electron – greatly reduces the statistical noise due to phonon fluctuations. In contrast, in the many-electron case, the fermionic and bosonic degrees of freedom are of similar importance, and world-line methods usually require the sampling of both, bosons and fermions [47]. Furthermore, world-line QMC methods with more than two electrons of different spin suffer from a severe sign problem in one (for periodic boundary conditions) and higher dimensions [39]. The polaron problem has also been investigated using a diagrammatic QMC approach [19, 20] originally

developed for the Fröhlich model which, given a convergent series of the polaron Green function, permits accurate calculations at zero temperature even in three dimensions [48].

In the present case, the Lang–Firsov transformation also yields a separation of polaron effects from the free-oscillator dynamics. However, the integral over the bosonic degrees of freedom is evaluated stochastically, thereby leaving us with a residual noise from the phonons. The numerical effort for calculations with our approach in the original form presented in [5] is proportional to LN^{3D}, while the checkerboard breakup yields a computer time $\propto LN^{2D}$. Nevertheless, our algorithm is not as efficient as the method of [13–16], in which the numerical effort is proportional to LD, the number of fermionic degrees of freedom [49].

The most time consuming calculations of this paper for two dimensions, $N = 12$, $\bar{\omega} = 0.1$ and $\lambda = 1$ took about 100 hours of CPU time on an Intel XEON 2600 MHz computer. To illustrate the advantage of the checkerboard breakup, we would like to mention that, using the full hopping term, the same simulation takes about 2500 hours. For less critical parameters, e.g., $\lambda = 2$, a similar accuracy of about 1% can be achieved within about 100 minutes. While a direct comparison with the calculations of de Raedt and Lagendijk [13–15] more than 20 years ago is not meaningful, Kornilovitch [16] reports simulation times of several hours on a workstation for a two-dimensional 32×32 cluster and similar accuracy. Thus, although our approach becomes increasingly slower with increasing system size compared to the methods of [13–18], it allows for accurate calculations on quite large systems with comparable CPU time in $D = 1$ and 2. Finally, we would like to mention that the present algorithm can easily be parallelized, since no warm-up phase is required, and measurements are completely independent.

5 Conclusions

The quantum Monte Carlo algorithm for the Holstein polaron proposed in [5] has been extended to higher dimensions. Additionally, a checkerboard breakup of the hopping term has been introduced, leading to a significant reduction of computer time, and results have been extrapolated in order to remove the error due to the Trotter decomposition. The method has been applied to calculate the electronic kinetic energy in one to three dimensions, and a very good agreement with existing work has been found.

While yielding results with the same or better accuracy over a very large range of parameters, the present approach is not quite as fast as other QMC methods for the Holstein polaron [13–18], the main limitation being the restriction to smaller but still reasonably large lattices. But remarkably, the current method can also be generalized to the many-electron case [8], in contrast to the world-line methods of [13–18].

Acknowledgements This work has been supported by the Austrian Science Fund (FWF), project No. P15834. One of us (M.H.) is grateful to the Austrian Academy of Sciences for financial support.

References

[1] Y. Bar-Yam, J. Mustre de Leon, and A. R. Bishop (eds.), Lattice Effects in High Temperature Superconductors (World Scientific, Singapore, 1992).
[2] D. M. Edwards, Adv. Phys. **51**, 1259 (2002).
[3] A. J. Millis, R. Mueller, and B. I. Shraiman, Phys. Rev. B **54**, 5405 (1996).
[4] E. Dagotto, S. Yunoki, and A. Moreo, in: Physics of Manganites, edited by T. A. Kaplan and S. D. Mahanti (Kluwer Publishing, New York, 1999), p. 39.
[5] M. Hohenadler, H. G. Evertz, and W. von der Linden, Phys. Rev. B **69**, 024301 (2004).
[6] I. G. Lang and Y. A. Firsov, Zh. Eksp. Teor. Fiz. **43**, 1843 (1962); Sov. Phys. JETP **16**, 1301 (1962).
[7] P. E. Kornilovitch and A. S. Alexandrov, Phys. Rev. B **70**, 224511 (2004).
[8] M. Hohenadler et al., cond-mat/0412010 (unpublished).
[9] M. Hohenadler and W. von der Linden, cond-mat/0409573; Phys. Rev. B (2005), accepted for publication.
[10] T. Holstein, Ann. Phys. (N.Y.) **8**, 325; **8**, 343 (1959).
[11] A. S. Alexandrov and N. Mott, Polaron & Bipolarons (World Scientific, Singapore, 1995).

[12] G. D. Mahan, Many-Particle Physics, 2nd ed. (Plenum Press, New York, 1990).
[13] H. De Raedt and A. Lagendijk, Phys. Rev. Lett. **49**, 1522 (1982).
[14] H. De Raedt and A. Lagendijk, Phys. Rev. B **27**, 6097 (1983).
[15] H. De Raedt and A. Lagendijk, Phys. Rev. B **30**, 1671 (1984).
[16] P. E. Kornilovitch, J. Phys.: Condens. Matter **9**, 10675 (1997).
[17] P. E. Kornilovitch, Phys. Rev. Lett. **81**, 5382 (1998).
[18] P. E. Kornilovitch, Phys. Rev. B **60**, 3237 (1999).
[19] N. V. Prokof'ev and B. V. Svistunov, Phys. Rev. Lett. **81**, 2514 (1998).
[20] A. S. Mishchenko, N. V. Prokof'ev, A. Sakamoto, and B. V. Svistunov, Phys. Rev. B **62**, 6317 (2000).
[21] H. Fehske, H. Röder, and G. Wellein, Phys. Rev. B **51**, 16 582 (1995).
[22] G. Wellein, H. Röder, and H. Fehske, Phys. Rev. B **53**, 9666 (1996).
[23] G. Wellein and H. Fehske, Phys. Rev. B **56**, 4513 (1997).
[24] W. Stephan, Phys. Rev. B **54**, 8981 (1996).
[25] M. Hohenadler, M. Aichhorn, and W. von der Linden, Phys. Rev. B **68**, 184304 (2003).
[26] E. Jeckelmann and S. R. White, Phys. Rev. B **57**, 6376 (1998).
[27] L. C. Ku, S. A. Trugman, and J. Bonča, Phys. Rev. B **65**, 174306 (2002).
[28] H. Sumi, J. Phys. Soc. Jpn. **36**, 770 (1974).
[29] S. Ciuchi, F. de Pasquale, S. Fratini, and D. Feinberg, Phys. Rev. B **56**, 4494 (1997).
[30] M. Capone, S. Ciuchi, and C. Grimaldi, Europhys. Lett. **42**, 523 (1998).
[31] S. Fratini, F. de Pasquale, and S. Ciuchi, Phys. Rev. B **63**, 153101 (2001).
[32] S. Fratini and S. Ciuchi, Phys. Rev. Lett. **91**, 256403 (2003).
[33] A. H. Romero, D. W. Brown, and K. Lindenberg, Phys. Lett. A **254**, 287 (1999).
[34] A. H. Romero, D. W. Brown, and K. Lindenberg, Phys. Rev. B **60**, 14080 (1999).
[35] V. Cataudella, G. De Filippis, and G. Iadonisi, Phys. Rev. B **60**, 15 163 (1999).
[36] R. R. dos Santos, Braz. J. Phys. **33**, 36 (2003).
[37] E. Y. Loh and J. E. Gubernatis, in: Electronic Phase Transitions, edited by W. Hanke and Y. V. Kopaev (Elsevier Science Publishers, North-Holland, Amsterdam, 1992), Chap. 4.
[38] M. Hohenadler, H. G. Evertz, and W. von der Linden, cond-mat/0401634 (unpublished).
[39] W. von der Linden, Phys. Rep. **220**, 53 (1992).
[40] M. Brunner, S. Capponi, F. F. Assaad, and A. Muramatsu, Phys. Rev. B **63**, R180511 (2001).
[41] M. Jarrell and J. E. Gubernatis, Phys. Rep. **269**, 133 (1996).
[42] E. V. L. de Mello and J. Ranninger, Phys. Rev. B **55**, 14 872 (1997).
[43] M. Hohenadler, Ph.D. thesis, Graz University of Technology, 2004.
[44] H. Lowen, Phys. Rev. B **37**, 8661 (1988).
[45] V. V. Kabanov and O. Y. Mashtakov, Phys. Rev. B **47**, 6060 (1993).
[46] H. Fehske, H. Röder, G. Wellein, and A. Mistriotis, Phys. Rev. B **51**, 16582 (1995).
[47] J. E. Hirsch and E. Fradkin, Phys. Rev. B **27**, 4302 (1983).
[48] A. S. Mishchenko et al., Phys. Rev. Lett. **91**, 236401 (2003).
[49] H. De Raedt and A. Lagendijk, Z. Phys. B, Condens. Matter **65**, 43 (1986).